Mansour Peimani[1]
Department of Electrical Engineering,
Science and Research Branch,
Islamic Azad University,
Tehran 1477893855, Iran
e-mail: m.peimani@srbiau.ac.ir

Mohammad Javad Yazdanpanah
Control and Intelligent Processing
Center of Excellence,
School of Electrical and Computer Engineering,
University of Tehran,
Tehran 1439957131, Iran
e-mail: yazdan@ut.ac.ir

Naser Khaji
Faculty of Civil and Environmental Engineering,
Tarbiat Modares University,
Tehran 14115-397, Iran
e-mail: nkhaji@modares.ac.ir

Adaptive Dynamic Surface Control of Bouc–Wen Hysteretic Systems

This paper develops an adaptive dynamic surface algorithm for designing the control law for uncertain hysteretic structural systems with seismic disturbances that can be converted to a semi strict feedback form. Hysteretic behavior is usually described by Bouc–Wen model for hysteretic structural systems like base isolation systems. Adaptive sliding mode and adaptive backstepping algorithms are also studied and simulated for comparison purposes. The presented simulation results indicate the effectiveness of the proposed control law in reducing displacement, velocity and acceleration responses of the structural system with acceptable control force. Moreover, using dynamic surface control (DSC), the study analyzes the stability of the controlled system based on the Lyapunov theory. [DOI: 10.1115/1.4033410]

1 Introduction

The protection of engineering structural systems from natural events is important specifically in the regions with high seismic activity. Control systems have been proposed to mitigate structural responses from dynamic loads. While the idea of structural control systems has been developed in a short time, the theoretical ideas have reached practical possibility [1–3]. The base isolation system is a useful mechanism for improving building structures response to dynamic excitation in seismic designs. An active base isolation system is defined by using an actuator, which provides the damping to the structure. The effectiveness of an active control strategy coupled with base isolation system has been shown in Ref. [4]. Active control systems operate by using an external energy supply where the control forces are applied by means of actuators. These can control the structural systems for a broader range of loadings, on the condition that it is technically feasible, and the required energy can be supplied [5].

Many physical systems and devices have hysteretic behavior as one of the most important existing nonlinearities. These systems may exhibit undesirable properties such as instability and oscillations. Thus, modeling and control of hysteretic systems have been one of the challenging issues, which have attracted attentions recently [6,7].

In structural control systems, the hysteretic behavior can be caused by the presence of isolation devices, bearings, semi-active magnetorheological (MR) dampers [8], or other hysteretic control devices. Moreover, Hysteretic behavior can be described by Bouc–Wen models [7,9,10]. The Bouc–Wen model has been used extensively to describe the hysteresis phenomenon in the areas of smart structures and civil engineering. It consists of a first-order nonlinear differential equation that relates the input displacement to the output restoring force in a rate-independent hysteretic way. The parameters that appear in the differential equation can be tuned to match the hysteresis loop of the system under study [9]. The system identification schemes have been developed for Bouc–Wen hysteretic systems [1–3]. Preliminary isolation systems have been applied in building structures to enhance the structural performance by reducing floor acceleration and decreasing force demand on superstructures [11,12].

The research on DSC has been developed extensively since 1997 [13–15]. DSC is an improved backstepping control (BSC) technique, and its design process is performed in a step-by-step style. A feedback controller is designed to guarantee the input-to-state stability of the corresponding subsystem at each step of the design. The primary advantage of DSC is to introduce a first-order and low-pass filter (LPF) of the synthetic input in which the problem of terms explosion, existing in the backstepping design approach, can be modified.

Recently, some researchers [6,14] have considered adaptive DSC (ADSC) of various nonlinear systems containing uncertain parameters. Moreover, the stability and performance for the DSC are tested numerically using a convex optimization tool in Ref. [16]. Zhang and Lin proposed a robust ADSC for a class of uncertain perturbed strict-feedback nonlinear systems with an unknown backlashlike hysteresis [17].

This study adopts the Bouc–Wen model in order to represent the hysteretic base-isolation system behavior. It has been previously indicated that the nonlinear part of the Bouc–Wen model is uniformly bounded while the upper bound could be derived as a definite function of the model parameters [18]. Numbers of control procedures for the hysteretic structural systems have been applied in theoretical researches [11,18]. But implementing an adaptive dynamic control system and analysing its performance have not been performed for a hysteretic structural system with the Bouc–Wen model representation. Thus, an active and adaptive controller is designed and used to reduce the effects of seismic excitation in order to stabilize the controlled system and improve the structural responses. In this paper, an ADSC is introduced and applied for seismic mitigation of a hysteretic structural system with unknown parameters. Hence, it could be considered as the first attempt to implement an ADSC method for unknown nonlinear systems having the Bouc–Wen hysteresis and dynamic uncertainties. Meanwhile, a comparison between the ADSC method over the adaptive BSC [18] and adaptive sliding mode control (SMC) [19] techniques has been performed and the advantages of the DSC to BSC and SMC are verified by simulation results.

[1]Corresponding author.

Contributed by the Dynamic Systems Division of ASME for publication in the Journal of Dynamic Systems, Measurement, and Control. Manuscript received July 26, 2015; final manuscript received April 4, 2016; published online June 6, 2016. Assoc. Editor: M. Porfiri.

Moreover, the stability of the closed-loop controlled system with proposed control law is proved and presented based on the Lyapunov theory.

2 DSC

The standard design procedure of the DSC to stabilize a Lipschitz nonlinear system was originally proposed by Swaroop et al. [14,16]. The class of nonlinear systems in strict feedback form is given by

$$\begin{aligned}\dot{x}_1 &= x_2 + f_1(x_1)\\ \dot{x}_2 &= x_3 + f_2(x_1, x_2)\\ &\vdots\\ \dot{x}_{n-1} &= x_n + f_{n-1}(x_1, ..., x_{n-1})\\ \dot{x}_n &= u + f_n(x_1, ..., x_n)\end{aligned} \tag{1}$$

where $x_1, x_2, ..., x_n$ are state variables, and $f_1, f_2, ..., f_n$ are the smooth functions. The first error surface is defined as

$$S_1 := x_1 - x_{1d} \tag{2}$$

where x_{1d} is the desired value. After taking the time derivative of S_1, the following relation is obtained:

$$\dot{S}_1 = x_2 + f_1(x_1) - \dot{x}_{1d} \tag{3}$$

Then the sliding condition, $S_1\dot{S}_1 < 0$ is satisfied if $x_2 = \bar{x}_2$ where

$$\bar{x}_2 = \dot{x}_{1d} - f_1(x_1) - K_1 S_1 \tag{4}$$

The next step is to make $x_2 \to \bar{x}_2$, so the second error surface is defined as

$$S_2 := x_2 - x_{2d} \tag{5}$$

where x_{2d} equals $\bar{x}_2$ passed through a first-order LPF as in Eq. (6)

$$\tau_2 \dot{x}_{2d} + x_{2d} = \bar{x}_2, \quad x_{2d}(0) := \bar{x}_2(0) \tag{6}$$

Carrying on with this process for $2 \le i \le n-1$

$$S_i := x_i - x_{id} \tag{7}$$

$$\bar{x}_{i+1} = \dot{x}_{id} - f_i(x_1, ..., x_i) - K_i S_i \tag{8}$$

where K_i are the controller gains. x_{i+1d} is obtained by filtering $\bar{x}_{i+1}$ as

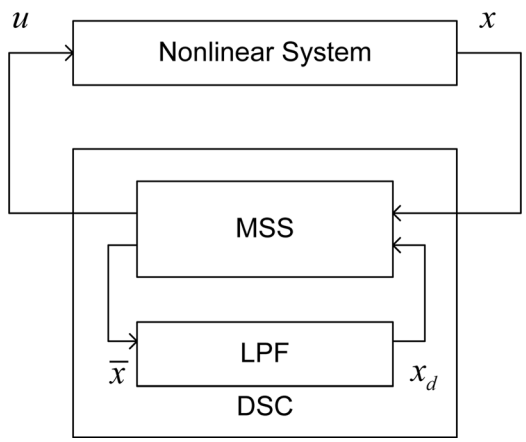

Fig. 1 Schematic representation of DSC

$$\tau_{i+1}\dot{x}_{i+1d} + x_{i+1d} = \bar{x}_{i+1}, \quad x_{i+1d}(0) := \bar{x}_{i+1}(0) \tag{9}$$

After continuing this procedure, Eqs. (10) and (11) are derived

$$S_n := x_n - x_{nd} \tag{10}$$

$$u = \dot{x}_{nd} - f_n(x_1, ..., x_n) - K_n S_n = \frac{\bar{x}_n - x_{nd}}{\tau_n} - f_n(x_1, ..., x_n) - K_n S_n \tag{11}$$

The structural design procedure for the DSC is shown in Fig. 1. DSC includes blocks of multiple sliding surface and LPF. These LPFs allow designing when the model is not differentiated, and the problem of "explosion of terms" could be solved [14]. The design procedure of DSC has been applied to a perturbed strict-feedback form (12) with unknown constant system parameters in Ref. [17]

$$\begin{aligned}\dot{x}_i &= g_i x_{i+1} + \theta_i f_i(\bar{x}_i) + \Delta_i(x,t),\ i = 1, ..., n-1\\ \dot{x}_n &= bu + \theta_n f_n(\bar{x}_n) + \Delta_n(x,t) + d_n\end{aligned} \tag{12}$$

where $\bar{x}_i = [x_1, x_2, ..., x_i]^{\mathrm{T}} \in \Re^i$, $i = 1, ..., n$ are the state vectors with $\bar{x}_n = x$, g_i, θ_i are unknown constant system parameters, Δ_i are unknown perturbed terms, d_n is a bounded disturbance term.

3 Hysteretic Structural System

Consider a nonlinear seismically excited base-isolation system as a hysteretic structural system, which is modeled as

$$m\ddot{x} + c\dot{x} + \Phi(x,t) = f(t) + u(t) \tag{13}$$

where m and c are the mass and the damping coefficients, respectively; Φ characterizes a nonlinear restoring force, where x gives the position, and $f(t)$ is a bounded unknown exciting force given by the earthquake ground acceleration and $u(t)$ is an active control force applied by suitable actuators. The hysteretic behavior can be due to the presence of passive rubber bearings, isolation devices, semi-active MR dampers, or hysteretic control devices. In Bouc–Wen model, the restoring force $\Phi(x,t)$ is represented by the superposition of an elastic element $\alpha_0 \kappa x(t)$ and a hysteresis element $(1-\alpha_0)D\kappa\omega(t)$ as

$$\Phi(x,t) = \alpha_0 \kappa x(t) + (1-\alpha_0)D\kappa\omega(t) \tag{14}$$

where $D > 0$ is the yield constant displacement and $\alpha_0 \in (0,1)$ is the post- to pre-yielding stiffness ratio. The hysteretic component involves a nondimensional auxiliary variable, $\omega(t)$, which is the solution of the nonlinear differential equation as follows:

$$\dot{\omega} = D^{-1}(A\dot{x} - \beta_0|\dot{x}||\omega|^{n-1}\omega - \lambda\dot{x}|\omega|^n) \tag{15}$$

where A, β_0, and λ are nondimensional parameters for controlling the shape and size of the transition from elastic to plastic response [18]. Figure 2 shows the sample hysteresis loop shapes with known base isolation parameters in Table 1.

The mechanical aspect of the problem is to design an active controller, which is supplied by appropriate actuators to decline the effect of an earthquake excitation. The effect of a base isolated system is to decrease the seismic lateral forces on a structure. This system isolates the shaking of the ground from the shaking of the structure and minimizes damage to the structure. It is the principle component in base isolation installed to provide passive and active protection of structures against earthquakes. The passive resistance is due to the physical design of the isolator between the base and the foundation. The active protection is added by a controller that provides forces generated by our designed feedback control law. Designing a DSC adaptive control law with

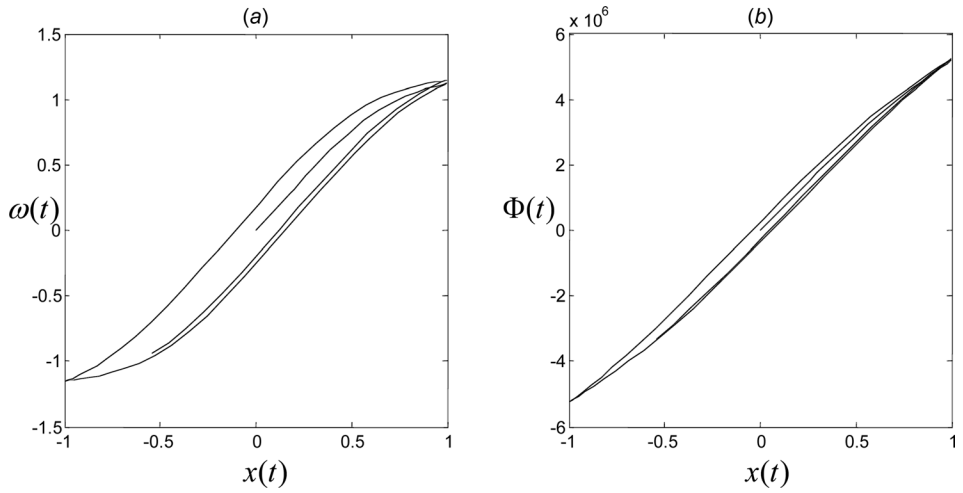

Fig. 2 (*a*) Variation of nondimensional auxiliary variable, $\omega(t)$ with respect to the position, $x(t)$. (*b*) Variation of restoring force, $\Phi(t)$ with respect to the position, $x(t)$.

closed-loop stability and small tracking error is the control objective in this paper.

4 Controller Design

In this section, an ADSC design is developed for a hysteretic structural system. Also, the adaptive laws of BSC and SMC for hysteretic systems have been reviewed.

4.1 ADSC Design for a Hysteretic System. The structural and isolation parameters are uncertain parameters. The residual effect of the hysteresis can be treated as a bounded disturbance with unknown bound. The bound involving the effect of the hysteresis and the external disturbance is estimated using an updating law. In this section, an ADSC technique is proposed to cope with the hysteretic structural system described by the perturbed strict-feedback form

$$\dot{x}_1 = x_2$$

$$\dot{x}_2 = \frac{1}{m}u(t) - \frac{c}{m}x_2 - \frac{\alpha_0\kappa}{m}x_1 + \frac{1}{m}\left[f(t) - \overbrace{(1-\alpha_0)D\kappa\omega(t)}^{R}\right] \tag{16}$$

where $x = [x_1, x_2]^{\mathrm{T}}$ is the state vector. The second equation of Eq. (16) can be written as $\dot{x}_2 = bu + \theta_2 f_2(x) + \Delta_2(x,t) + d_2$ where $d_2 = (1/m)[f - R]$ denotes a bounded disturbance term satisfying $|d_2| < d$, because $|f(t)| \le F$, $R \le (1-\alpha_{\min})D_{\max}\kappa_{\max}\max|\omega(t)|$, and $\max|\omega(t)|$ exists and its upper bound can be determined.

The output $\omega(t)$ is uniformly bounded if the parameters of the system (15) verify the inequalities in Table 2, for any bounded or unbounded piecewise continuous signals x and $\dot{x}$ based on the proposed theorem in Ref. [18]. The variables ω_0 and ω_1 are defined as $\omega_0 = \sqrt[n]{A/(\beta+\lambda)}$ and $\omega_1 = \sqrt[n]{A/(\lambda-\beta_0)}$. These variables are used in Table 2 for specifying the output signal and initial condition bounds. The proof of this theorem is given in Refs. [18] and [20].

$b = 1/m$, $\theta_2 = c/m$, and $d_{2\max}$ are unknown constant system parameters, and they will be estimated online. $f_2(x) = -x_2$ is a known smooth function. $\Delta_2(x,t) = -\alpha_0 k x_1/m$ is a disturbance term satisfies Eq. (17)

$$\left|\Delta_2(x,t)\right| \le \rho_2(x) = \frac{\alpha_{\max}\kappa_{\max}}{m_{\min}}x_1 \tag{17}$$

There are two steps in the design procedure. The actual control law u is deduced in the second step.

Step 1. The first surface error is defined as $S_1 = x_1$. To meet our control objective. the desired state variable x_{1d} is set to zero, then

$$\dot{S}_1 = \dot{x}_1 = x_2 \tag{18}$$

A virtual control signal is chosen based on Eq. (18) as

$$\bar{x}_2 = -k_1 S_1 \tag{19}$$

Let $\bar{x}_2$ pass through a first-order filter to obtain x_{2d} as

$$\tau_2\dot{x}_{2d} + x_{2d} = \bar{x}_2, \quad x_{2d}(0) = \bar{x}(0) \tag{20}$$

where τ_2 is the time constant.

Step 2. The second surface error is defined as $S_2 = x_2 - x_{2d}$, then

$$\dot{S}_2 = \dot{x}_2 - \dot{x}_{2d} = bu + \theta_2 f_2(x) + \Delta_2(x,t) + d_2 - \dot{x}_{2d} \tag{21}$$

Table 1 Parameters of the hysteretic system

Parameter	Description	Value for the system
m	Mass ($\times$1000 kg)	156
k	Stiffness ($\times$1000 N/m)	6000
c	Damping ($\times$1000 N s/m)	20
α_0	Stiffness ratio	0.6
D	Yield constant displacement (m)	0.6
A, β_0, λ	Control the shape and size of the hysteresis	1, 0.1, 0.5
n	Smoothness	3

Table 2 Boundedness of the hysteretic part of the Bouc–Wen model

Case		Ω	$\lvert\omega(t)\rvert$ bound
$A > 0$	$\beta_0+\lambda > 0$ and $\beta_0-\lambda \ge 0$	$\Re$	$\max(\lvert\omega_0\rvert, \omega_0)$
	$\beta_0-\lambda < 0$ and $\beta_0 \ge 0$	$[-\omega_1, \omega_1]$	$\max(\lvert\omega_0\rvert, \omega_0)$
$A < 0$	$\beta_0-\lambda > 0$ and $\beta_0+\lambda \ge 0$	$\Re$	$\max(\lvert\omega_0\rvert, \omega_1)$
	$\beta_0+\lambda < 0$ and $\beta_0 \ge 0$	$[-\omega_0, \omega_0]$	$\max(\lvert\omega_0\rvert, \omega_1)$
$A = 0$	$\beta_0+\lambda \ge 0$ and $\beta_0-\lambda \ge 0$	$\Re$	$\lvert\omega_0\rvert$
Other cases		$\varnothing$	

Let $\zeta = 1/b$, then the control law is designed as $u = \hat{\zeta}\bar{u}$. $\hat{\zeta}$ is the estimate of ζ, and it is updated by $\dot{\hat{\zeta}} = -\gamma_\zeta(\bar{u}S_2 + \eta_\zeta\hat{\zeta})$. γ_ζ and η_ζ are positive design parameters, and

$$\bar{u} = -k_2 S_2 - \hat{\theta}_2 f_2(x) - S_2\rho_2^2(x)/2\varepsilon + \dot{x}_{2d} - \mathrm{sgn}(S_2)\hat{d} \tag{22}$$

where ε is any positive constant. $\hat{\theta}_2$ and $\hat{d}$, which are the estimations of θ_2 and d, respectively, are updated by Eqs. (23) and (24)

$$\dot{\hat{\theta}}_2 = \gamma_2(f_2(x)S_2 - \eta_2\hat{\theta}_2) \tag{23}$$

$$\dot{\hat{d}} = \gamma_d(|S_2| - \eta_d\hat{d}) \tag{24}$$

4.2 Adaptive BSC Law for a Hysteretic System. The adaptive BSC law (25) and parameter estimation laws (26) in Ref. [18] are considered for simulation, calculating evaluation criteria, and comparison with our proposed ADSC in this paper

$$u(t) = -\hat{\theta}^T\varphi - c_1\frac{v}{d}(x_2 - \dot{y}_r)\hat{m} - \frac{v^2}{d^2}\hat{m}z_1 - \frac{d}{v^3 m_{\max}}d_2 z_2 r^2 + \hat{m}\ddot{y}_r - \frac{v m_{\max}}{d}c_2 z_2 - sg\left(\frac{z_2}{v}\right)cf\left(\frac{|z_2|}{v}\right)gF$$

$$\dot{\hat{\theta}} = \frac{M_\theta^2}{m_{\max}v^2}\Gamma\varphi z_2 - \frac{v}{d}\Gamma\sigma_\theta\left(\|\hat{\theta}\|/M_\theta\right)\hat{\theta}$$

$$\dot{\hat{m}} = \gamma m_{\max}\left(\frac{c_1}{dv}x_2 + \frac{1}{d^2}z_1 - \frac{1}{v^2}\ddot{y}_r - \frac{c_1}{dv}\dot{y}_r\right)z_2 - \gamma\frac{v}{d}\sigma_m\left(\frac{|\hat{m}|}{m_{\max}}\right)\hat{m}$$

$$cf(y) = \sigma(y/\varepsilon_1)$$

$$\sigma_\theta(y) = \bar{\sigma}_\theta\sigma(y)$$

$$\sigma_m(y) = \bar{\sigma}_m\sigma(y)$$

$$\sigma(y) = \begin{cases} 0, & y \le 1 \\ y-1, & y \in [1,2] \\ 1, & y \ge 2 \end{cases} \quad sg(y) = \begin{cases} -1, & y \le -\varepsilon_2 \\ \dfrac{1}{\varepsilon_2}y, & y \in [-\varepsilon_2, \varepsilon_2] \\ 1, & y \ge \varepsilon_2 \end{cases} \tag{26}$$

where c_1, c_2, d_2, g, Γ, $\bar{\sigma}_\theta$, $\bar{\sigma}_m$, and ε_1 are design parameters. θ is the constant vector of uncertain parameters and φ is the regression vector. The adaptive BSC law involves model differentiations and terms explosion but DSC law prevents this problem [14].

4.3 Adaptive SMC Law for a Hysteretic System. SMC systems have been known to be robust in the presence of perturbations [19]. Considering the sliding surface in Eq. (27) and the adaptive law (28) and (29) the controlled system in Eq. (16) converges to the sliding surface $s(t) = 0$. The modification in Eq. (30) can be used in the practical implementation [19]

$$s(x_1, x_2) = x_2 + \alpha x_1 \tag{27}$$

$$u = -m\left[\left(\alpha_0 - \frac{c}{m}\right)x_2 - \frac{\alpha_0 k}{m}x_1 + (\eta + \hat{\beta})\mathrm{sgn}(s)\right] \tag{28}$$

$$\dot{\hat{\beta}} = |s|,\ \hat{\beta}(0) \ge 0 \tag{29}$$

$$\dot{\hat{\beta}} = -\nu\hat{\beta} + |s| \tag{30}$$

5 Stability Analysis

The analysis of stability and transient performance of the proposed DSC scheme, which develops the techniques given by Refs. [14] and [17], will be presented in this section. Although the design procedure is simple, the derivation of the LPFs makes the stability analysis complicated. To this aim, define y_2 as

$$y_2 = x_{2d} - \bar{x}_2 = x_{2d} + k_1 S_1 \tag{31}$$

where $\bar{x}_2$ is given by Eq. (19). Further, define the estimation errors as

$$\tilde{\theta}_2 = \hat{\theta}_2 - \theta_2,\ \tilde{\zeta} = \hat{\zeta} - \zeta,\ \tilde{d} = \hat{d} - d \tag{32}$$

Using Eqs. (31) and (32), we can write Eq. (18) as

$$\dot{S}_1 = -k_1 S_1 + S_2 + y_2 \tag{33}$$

We can rewrite bu in Eq. (21) as

$$bu = b\hat{\zeta}\bar{u} = b(\tilde{\zeta} + \zeta)\bar{u} = b\tilde{\zeta}\bar{u} + \bar{u} \tag{34}$$

Taking Eqs. (22), (32), and (34) into consideration, Eq. (21) can be rewritten as

$$\dot{S}_2 = -k_2 S_2 - \tilde{\theta}_2 f_2(x) + (\Delta_2 - S_2\rho_2^2(x)/2\varepsilon) + d_2 - \mathrm{sgn}(S_2)\hat{d} + b\tilde{\zeta}\bar{u} \tag{35}$$

Since $\dot{x}_{2d} = \bar{x}_2 - x_{2d}/\tau_2 = -y_2/\tau_2$. From Eq. (19), we obtain

$$\dot{y}_2 = -y_2/\tau_2 + k_1\dot{S}_1 = -y_2/\tau_2 + B_2 \tag{36}$$

where B_2 is a continuous function.

THEOREM. *Consider the closed-loop system* (16), (33), (35), *and* (36). *Let the Lyapunov function candidate be defined as*

$$V = \frac{1}{2}\left(S_1^2 + y_2^2 + S_2^2 + \frac{b}{\gamma_\zeta}\tilde{\zeta}^2 + \frac{1}{\gamma_{\theta 2}}\tilde{\theta}_2^2 + \frac{1}{\gamma_d}\tilde{d}^2\right) \tag{37}$$

Then for any given positive number ρ, if $V(0) \le \rho$, there exists design parameters, $k_1, k_2, \tau_2, \gamma_\zeta, \gamma_{\theta 2}, \gamma_d, \eta_\zeta, \eta_\theta, \eta_d$, such that all the closed-loop signals are uniformly bounded and the tracking error converges to a residual set that can be made arbitrarily small by appropriate choosing of the design parameters. The proof of the theorem is presented in this section.

Proof. The time derivative of V yields

$$\dot{V} = S_1\dot{S}_1 + y_2\dot{y}_2 + S_2\dot{S}_2 + b\tilde{\zeta}\dot{\tilde{\zeta}}/\gamma_\zeta + \tilde{\theta}_2\dot{\tilde{\theta}}_2/\gamma_{\theta 2} + \tilde{d}\dot{\tilde{d}}/\gamma_d \tag{38}$$

The inequalities $S_2\Delta_2 \le |S_2|\rho_2(x) \le S_2^2\rho_2^2(x)/2\varepsilon + \varepsilon/2$ hold. Using Eq. (33), it is obtained that

$$S_1\dot{S}_1 \le (-k_1 S_1^2 + S_1 S_2 + S_1 y_2 + S_1 c_2 + \dot{y}_r S_1 + \varepsilon/2) \tag{39}$$

Moreover, using Eq. (35), it is obtained that

$$S_2\dot{S}_2 \le (-k_2 S_2^2 + b\tilde{\zeta}\bar{u}S_2 + S_2 d - |S_2|\hat{d} - \tilde{\theta}_2 f_2(x)S_2 + \varepsilon/2) \tag{40}$$

In view of Eqs. (36), (39), (40) and substituting the adaptive laws into Eq. (38) yields

$$\dot{V} \le -k_1 S_1^2 + S_1 S_2 + S_1 y_2 - k_2 S_2^2 - \eta_\zeta b\hat{\zeta}\tilde{\zeta} - \eta_d\hat{d}\tilde{d} - \eta_\theta\hat{\theta}\tilde{\theta} - y_2^2/\tau_2 + |y_2 B_2| + \varepsilon \tag{41}$$

Consider the sets $Q = \{(y_r, \dot{y}_r, \ddot{y}_r) : y_r + \dot{y}_r + \ddot{y}_r \le B_1\}$, $Q_1 = \{S_1^2 + y_2^2 \le 2p\}$, and $Q_2 = \{S_1^2 + y_2^2 + b\tilde{\zeta}^2/\gamma_\zeta + \tilde{\theta}_2^2/\gamma_{\theta 2} + \tilde{d}^2/\gamma_d + S_2^2 \le 2p\}$ which are compact in $\Re^3$, $\Re^2$, and $\Re^6$. Therefore, $|B_2|$ have maximum, i.e., M_2 on $Q \times Q_1$. Using the inequalities $S_1 S_2 \le S_1^2 + S_2^2/4$ and $S_1 y_2 \le S_1^2 + y_2^2/4$, we have

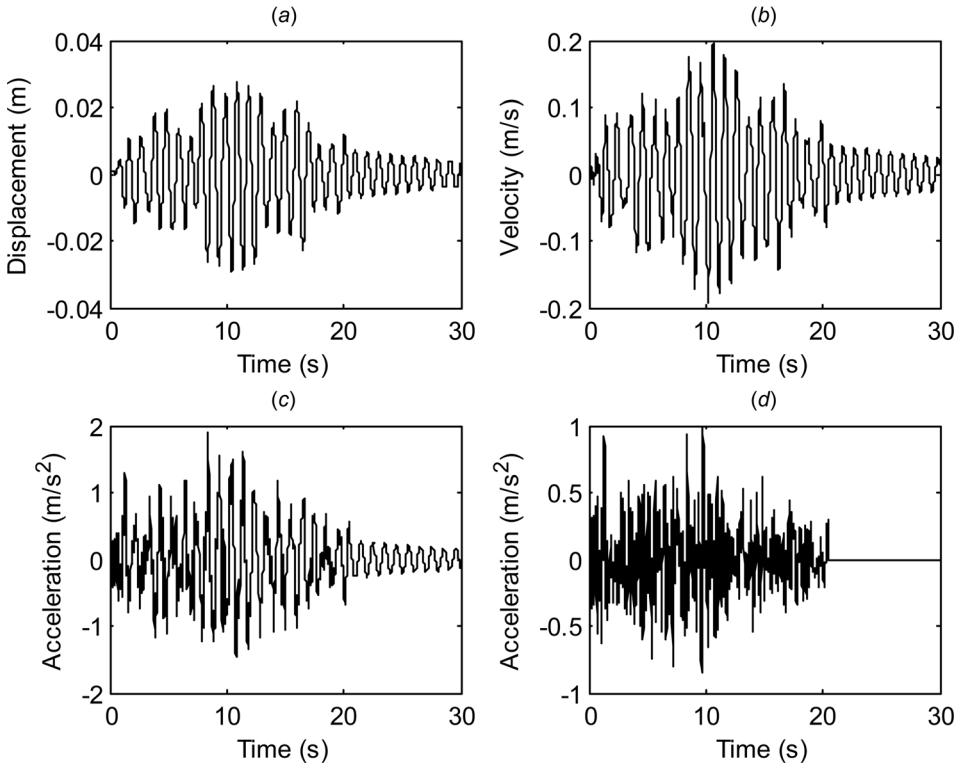

Fig. 3 Time responses of the uncontrolled hysteretic structure: (*a*) displacement, (*b*) velocity, (*c*) acceleration, and (*d*) Taft earthquake acceleration record

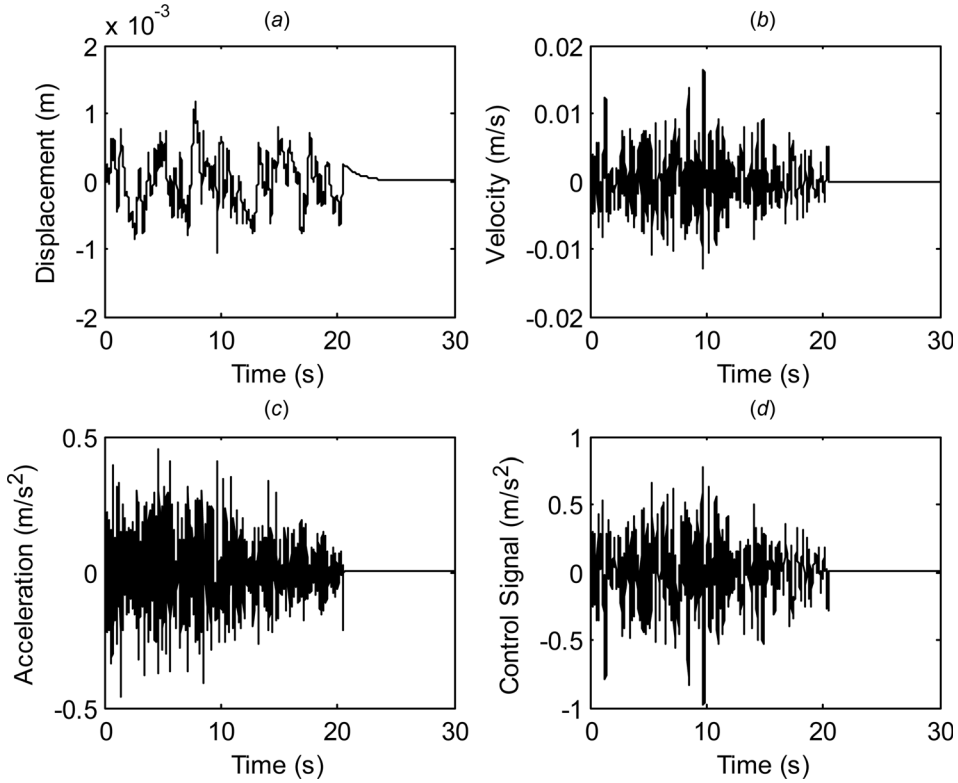

Fig. 4 Time histories of the controlled system using ADSC: (*a*) displacement, (*b*) velocity, (*c*) acceleration, and (*d*) Control signal (acceleration, $u(t)/m$)

$$\dot{V} \le -k_1 S_1^2 + 3S_1^2 + S_2^2/4 + y_2^2/4 - k_2 S_2^2 - \eta_\zeta b\hat{\zeta}\tilde{\zeta} - \eta_d \hat{d}\tilde{d} - \eta_2 \hat{\theta}_2 \tilde{\theta}_2 - y_2^2/\tau_2 + |y_2 B_2| + \varepsilon \quad (42)$$

In the inequality (42), $k_1 = 3 + a$, $k_2 = 1/4 + a$, $\eta_2 = 2a/\gamma_{\theta 2}$, $\eta_\zeta = 2a/\gamma_\zeta$, $\eta_d = 2a/\gamma_d$ in which a is a positive constant. Also, note that $\hat{\zeta}\tilde{\zeta} = \tilde{\zeta}^2 + \zeta\tilde{\zeta}$, $\hat{d}\tilde{d} = \tilde{d}^2 + d\tilde{d}$ and $\hat{\theta}_2\tilde{\theta}_2 = \tilde{\theta}_2^2 + \theta_2\tilde{\theta}_2$. Hence, the following inequalities hold:

$$-\eta_\zeta b\tilde{\zeta}\hat{\zeta} \le -\eta_\zeta b(\tilde{\zeta}^2 - \zeta^2)/2, -\eta_d \tilde{d}\hat{d} \le -\eta_d(\tilde{d}^2 - d^2)/2, \quad -\eta_{\theta 2}\tilde{\theta}_2\hat{\theta}_2 \le -\eta_{\theta 2}(\tilde{\theta}_2^2 - \theta_2^2)/2 \quad (43)$$

From Eqs. (42) and (43), we obtain that

$$\dot{V} \le -aS_1^2 - a(b\tilde{\zeta}^2/\gamma_\zeta + \tilde{\theta}_2^2/\gamma_{\theta 2} + b\tilde{d}^2/\gamma_d) + (y_2^2/4 - y_2^2/\tau_2 + |y_2 B_2|) + \eta_2\theta_2^2/2 + \eta_\zeta b\zeta^2/2 + \eta_d d^2/2) + \varepsilon \quad (44)$$

We have $|y_2 B_2| \le y_2^2 M_2^2/2\mu + \mu/2$ for any positive number μ. Let $1/\tau_2 = 1/4 + M_2^2/2\mu + a$, $e_M = \eta_2\theta_2^2/2 + \eta_\zeta b\zeta^2/2 + \eta_d d^2/2 + \varepsilon$, then we have the following inequality:

$$y_2^2/4 - y_2^2/\tau_2 + |y_2 B_2| \le -ay_2^2 + \mu/2 \quad (45)$$

Replacing Eq. (45) in Eq. (44), it follows that:

$$\dot{V} \le -2aV + e_M + \mu/2 \quad (46)$$

Let $a > (e_M + \mu/2)/2p$ then $\dot{V} \le 0$ on $V = p$. That is, $V \le p$ is an invariant set, i.e., if $V(0) \le p$, then $V(t) \le p$, for all $t \ge 0$. Solving the inequality (46), we obtain

$$V(t) \le (e_M + \mu/2)/2a + (V(0) - (e_M + \mu/2)/2a)e^{-2at} \quad (47)$$

which implies that $\lim_{t\to\infty} V(t) = (e_M + \mu/2)/2a$. Thus, all closed-loop signals are uniformly bounded.

6 Results and Discussion

The objectives for structural control systems are reducing structural responses such as displacement and acceleration in the base level and thus, making the base isolator work in its elastic region. Also, decoupling the dynamic movement of the main structure from the base motion is desired in these systems [21].

In this section, the effectiveness of seismic mitigation using ADSC has been demonstrated through numerical simulations. The parameter values for the hysteretic system are taken from Ref. [18] and are shown in Table 1. The possible changes of the structural parameters could be due to the effect of likely faults in the base isolation system. The constant values given in Table 1 are chosen as the true nominal parameters for the hysteretic system. It is not required to know the exact values of these parameters to implement the adaptive controllers. Also, the initial values of the system parameters are different from their true nominal values.

The reference trajectory is set to zero, because the control objective is to mitigate the seismic response of the system. The selected values for the set of DSC parameters are $k_1 = k_2 = \tau_2 = \eta_2 = \eta_\xi = \eta_d = \varepsilon = 0.01$ and $\gamma_{\theta 2} = \gamma_d = 1$. Increasing the surface gains makes the system more robust. Also, increasing the control gains and time constants makes the closed-loop system unstable. Accordingly, a systematic method for choosing appropriate gains and filter time constants for a DSC has not been fully addressed yet in the literature [16]. However, better performance with acceptable control effort is the criterion of parameter tuning in this research.

Taft earthquake is considered as the external excitation in this paper. Taft Lincoln station is in Kern Country and its moment magnitude is 7.4, and its peak ground acceleration is 0.1 g. The earthquake record is available in Pacific Earthquake Engineering Research Center: NGA Database. Also, Taft seismic was used as a standard earthquake which was used in Ref. [18] and the time history of the acceleration of this earthquake is illustrated in Fig. 3. The simulation parameters for ASMC are $\alpha = 0.5$, $\eta = 0.1$, $\nu = 1$. The parameter values for adaptive BSC and adaptive SMC are chosen as in Refs. [18] and [19] and so the chosen parameters would enable a fair control performance comparison between ADSC and other two approaches as seen in simulation results.

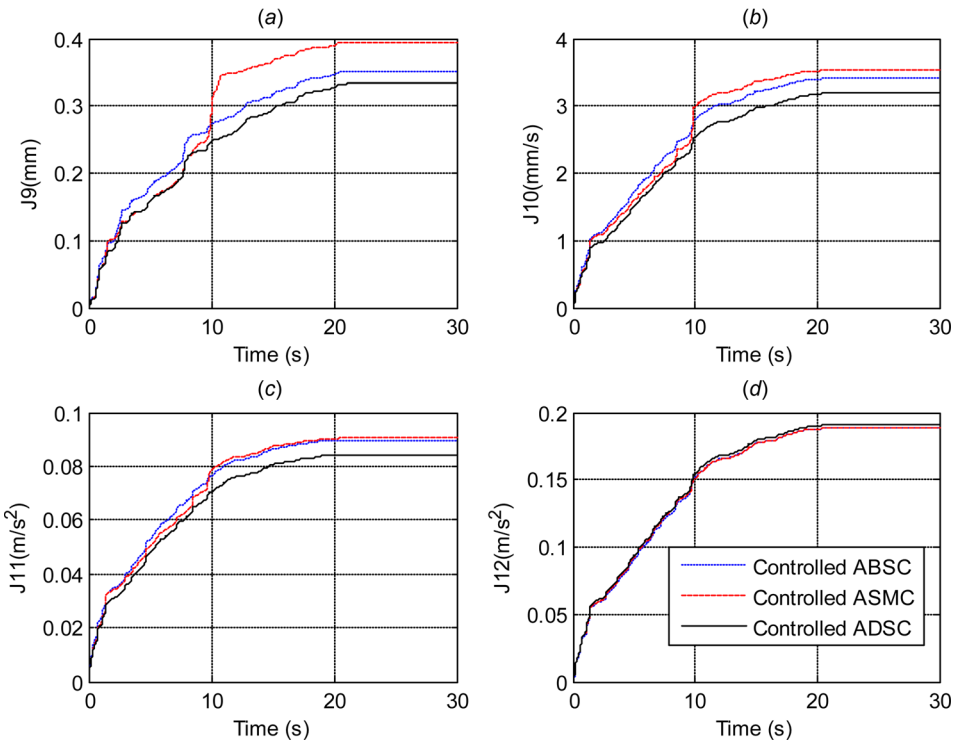

Fig. 5 Performance criteria $J_9 - J_{12}$

Table 3 Performance criteria for controlled and uncontrolled systems

Criteria	Units	Uncontrolled	Adaptive SMC	Adaptive BSC	ADSC
$J_1 = \max(\lvert x(t)\rvert)$	mm	29.43	1.89	1.29	1.18
$J_2 = \max(\lvert \dot{x}(t)\rvert)$	mm/s	195.96	29.68	17.27	16.32
$J_3 = \max(\lvert \ddot{x}(t)\rvert)$	m/s^2	1.89	0.69	0.50	0.45
$J_4 = \max(\lvert u(t)\rvert/m)$	m/s^2	0	0.63	0.96	0.97
$J_5 = (\frac{1}{T}\int_0^t x^2(t)dt)^{1/2}$	mm	10.89	0.39	0.35	0.33
$J_6 = (\frac{1}{T}\int_0^t \dot{x}^2(t)dt)^{1/2}$	mm/s	68.42	3.53	3.41	3.19
$J_7 = (\frac{1}{T}\int_0^t \ddot{x}^2(t)dt)^{1/2}$	m/s^2	0.47	0.09	0.09	0.08
$J_8 = (\frac{1}{T}\int_0^t (u(t)/m)^2dt)^{1/2}$	m/s^2	0	0.19	0.19	0.19

Displacement, velocity, and acceleration responses of the uncontrolled and controlled systems using proposed DSC are illustrated in Figs. 3 and 4. Considerable reductions are seen for the controlled system in comparison with the uncontrolled cases in Fig. 3.

After $t = 20$ s, the excitation stops, and the uncontrolled cases correspond to the free vibration responses. The open-loop system exhibits a light damping behavior, but the proposed control drives the response toward zero rapidly, and introduces a significant damping effect into the controlled system. Comparing with the other methods, controlled system performance is improved for DSC, and a reduction in the magnitude of displacement, velocity, and acceleration can be observed for DSC.

A set of performance criteria [22] is used here for comparing the controlled and uncontrolled cases. $J_1 - J_4$ are, respectively, defined as the maximum peak values of absolute displacement, velocity, acceleration and control signal $(u(t)/m)$. $J_5 - J_8$ are defined as the RMS values for the absolute displacement, velocity, acceleration and control signal, respectively.

Results of the measured performance criteria for the uncontrolled and controlled cases are presented in Table 3. The reduction is seen in displacement, velocity and acceleration of the controlled structure in comparison with the uncontrolled structure in both viewpoints of the maximum peak and root-mean-square (RMS) values. When the adaptive BSC is compared with the DSC, the DSC outperforms adaptive backstepping in all performance criteria. The maximum absolute J_4 and RMS value J_8 of the control signals are almost the same for two DSC and BSC control techniques. These indices are related to the control effort but not direct indicator of energy consumption of the control system.

Furthermore, four new performance criteria are defined to provide a better comparison

$$J_9 = \left(\frac{1}{T}\int_0^t x^2(t)dt\right)^{1/2},\ J_{10} = \left(\frac{1}{T}\int_0^t \dot{x}^2(t)dt\right)^{1/2},$$
$$J_{11} = \left(\frac{1}{T}\int_0^t \ddot{x}^2(t)dt\right)^{1/2},\ J_{12} = \left(\frac{1}{T}\int_0^t u^2(t)dt\right)^{1/2} \quad (48)$$

These indices are used to consider the RMS values of the response and control signal for each time of the simulation. The indices J_9, J_{10}, and J_{11} are illustrated in Figs. 5(*a*)–5(*c*) for different control methods. The indices for the DSC have the lowest values as compared to the other methods which show the better performance of the DSC. Figure 5(*d*) shows the control effort of the different control methods. The control effort of BSC and SMC are slightly less than DSC method as seen in Fig. 5(*d*), instead the performance criteria for displacement, velocity, and acceleration responses are reduced significantly as seen in Figs. 5(*a*)–5(*c*).

7 Conclusions

The design procedure and implementation of the ADSC for a hysteretic structural system have been presented in this paper. The controller design utilizes the first-order and LPFs to avoid model differentiations, and it overcomes the problem of terms explosion of the adaptive backstepping approach. The results of the study indicate that the presented control law can stabilize the controlled system based on the Lyapunov theory. Considering simulation results and some performance criteria, the proposed control law is effective in reducing displacement, velocity and acceleration responses of the hysteretic structural system in comparison to the backstepping and sliding mode techniques.

References

[1] Peimani, M., Yazdanpanah, M. J., and Khaji, N., 2013, "Parameter Estimation in Hysteretic Systems Based on Adaptive Least-Squares," J. Inf. Syst. Telecommun., **1**(4), pp. 217–221.

[2] Mu, T., Zhou, L., and Yang, J. N., 2013, "Comparison of Adaptive Structural Damage Identification Techniques in Nonlinear Hysteretic Vibration Isolation Systems," Earthquake Eng. Eng. Vib., **12**(4), pp. 659–667.

[3] Zhang, J., Sato, T., Iai, S., and Hutchinson, T., 2008, "A Pattern Recognition Technique for Structural Identification Using Observed Vibration Signals: Nonlinear Case Studies," Eng. Struct., **30**(5), pp. 1417–1423.

[4] DeVore, C., Chang, C.-M., and Spencer, Jr., B., 2007, "Active Base Isolation of Building Structures in Two Dimensions," Earthquake Engineering Symposium for Young Researchers, pp. 1–10.

[5] Maldonado-Mercado, J. C., 1995, "Passive and Active Control of Structures," Doctoral dissertation, Massachusetts Institute of Technology, Cambridge, MA.

[6] Zhang, T. P., and Ge, S. S., 2008, "Adaptive Dynamic Surface Control of Nonlinear Systems With Unknown Dead Zone in Pure Feedback Form," Automatica, **44**(7), pp. 1895–1903.

[7] Kottari, A. K., Charalampakis, A. E., and Koumousis, V. K., 2014, "A Consistent Degrading Bouc–Wen Model," Eng. Struct., **60**, pp. 235–240.

[8] Tsang, H. H., Su, R. K. L., and Chandler, A. M., 2006, "Simplified Inverse Dynamics Models for MR Fluid Dampers," Eng. Struct., **28**(3), pp. 327–341.

[9] Ikhouane, F., and Rodellar, J., 2007, *Systems With Hysteresis: Analysis, Identification and Control Using the Bouc–Wen Model*, Wiley, UK.

[10] Ismail, M., Rodellar, J., and Ikhouane, F., 2010, "An Innovative Isolation Device for Aseismic Design," Eng. Struct., **32**(4), pp. 1168–1183.

[11] Zhou, J., Wen, C., and Cai, W., 2006, "Adaptive Control of a Base Isolated System for Protection of Building Structures," ASME J. Vib. Acoust., **128**(2), pp. 261–268.

[12] Etedali, S., Sohrabi, M. R., and Tavakoli, S., 2013, "Optimal PD/PID Control of Smart Base Isolated Buildings Equipped With Piezoelectric Friction Dampers," Earthquake Eng. Eng. Vib., **12**(1), pp. 39–54.

[13] Wei, D. Q., Luo, X. S., Wang, B. H., and Fang, J. Q., 2007, "Robust Adaptive Dynamic Surface Control of Chaos in Permanent Magnet Synchronous Motor," Phys. Lett. A, **363**(1–2), pp. 71–77.

[14] Swaroop, D., Hedrick, J. K., Yip, P. P., and Gerdes, J. C., 2000, "Dynamic Surface Control for a Class of Nonlinear Systems," IEEE Trans. Autom. Control, **45**(10), pp. 1893–1899.

[15] Swaroop, D., Gerdes, J. C., Yip, P. P., and Hedrick, J. K., 1997, "Dynamic Surface Control of Nonlinear Systems," American Control Conference, pp. 3028–3034.

[16] Song, B., and Hedrick, J. K., 2011, *Dynamic Surface Control of Uncertain Nonlinear Systems*, Springer, London.

[17] Zhang, X. Y., and Lin, Y., 2010, "A Robust Adaptive Dynamic Surface Control for Nonlinear Systems With Hysteresis Input," Zidonghua Xuebao/Acta Autom. Sin., **36**(9), pp. 1264–1271.

[18] Ikhouane, F., Manosa, V., and Rodellar, J., 2005, "Adaptive Control of a Hysteretic Structural System," Automatica, **41**(2), pp. 225–231.

[19] Acho, L., and Pozo, F., 2009, "Sliding Mode Control of Hysteretic Structural Systems," Int. J. Innovative Comput. Inf. Control, **5**(4), pp. 1081–1087.

[20] Khalil, H. K., and Grizzle, J. W., 1996, *Nonlinear Systems*, Prentice Hall, Upper Saddle River, NJ, Vol. 3.

[21] Zapateiro, M., Karimi, H. R., and Luo, N., 2011, "Semiactive Vibration Control of Nonlinear Structures Through Adaptive Backstepping Techniques With H_∞ Performance," Int. J. Syst. Sci., **42**(5), pp. 853–861.

[22] Wang, S. G., Roschke, P. N., and Yeh, H. Y., 2004, "Robust Control for Structural Systems With Unstructured Uncertainties," J. Eng. Mech., **130**(3), pp. 337–346.